VSOP-2 SCIENCE CASE

S. Kameno[(1)] and VSOP-2 Science Working Group

[(1)]National Astronomical Observatory of Japan, 2-21-1 Osawa, Mitaka, Tokyo 181-8588 Japan

Abstract. VSOP-2 is a space VLBI project, following the VSOP (VLBI Space Observatory Programme), organized by the space VLBI working group consisting of the Japan Aerospace Exploration Agency (JAXA), the National Astronomical Observatory of Japan (NAOJ), and the university interest group. We aim synthesis imaging with the angular resolutions of 38, 75, and 205 microarcsec at 43, 22, and 8 GHz, respectively, to unveil extremely compact celestial objects. Phase referencing capability, 1-Gbps wideband downlink, and cooled dual polarization receivers will be able to provide high sensitivity, with the minimum detectable brightness temperature of a few 10^8 K. Dual polarization observations are supported for 4-Stokes-parameter imaging. The VSOP-2 science working group have continued discussion on VSOP-2 science case. The main astronomical targets are active galactic nuclei (AGNs) and young stellar objects (YSOs). VSOP-2 will image accretion disks, roots of jets, and circumnuclear regions of nearby AGNs with a resolution of $\sim$ 10 Schwarzschild radii. It also allows us to investigate magnetospheres, protoplanetary disks, and roots of outflows of YSOs with a resolution of $\sim$ 1 solar radius in nearby star-forming regions.

1. Active Galactic Nuclei

AGNs are the most powerful engines in the universe, which emit $\sim 10^{33} - 10^{41}$ W ($\sim 10^6 - 10^{14}$ $L_\odot$). Their power source is considered to be gravitational energy of accreting matter into a black hole. A massive black hole at the heart of galaxies digs a deep gravitational potential well. When a tiny piece of gas in a galactic disk is swallowed into the well, it forms an accretion disk, get heated, and shine at very hot temperature. The accretion energy is converted to radiative emission, advection into the black hole, and kinetic energy of jets. The jet is a bipolar flow of relativistic plasma emanating from the central engine and reachable to Mpc scale. The flow terminates at hot spots and spread out as radio lobes.

1.1. Black Holes

Black hole sizes are characterized by the Schwarzschild radius, r_s, which is given by $r_s = \frac{2GM_{\rm BH}}{c^2}$, where c is the speed of light, $M_{\rm BH}$ is the black hole mass, and G is the gravity constant. For a massive AGN with $M_{\rm BH} = 10^9$ $M_\odot$, for instance, the Schwarzschild radius is 20 AU and its apparent size will be 2 μas if the distance is 10 Mpc. M 87 is the most preferable candidate for black hole imaging. Its apparent shadow diameter is expected to be 26 μas, which is comparable to the VSOP-2 resolution, as shown in figure 1 (Takahashi 2004). It is still unclear how bright is the background and how much does plasma defocus, nevertheless, VSOP-2 is the best telescope to approach the direct image of a black hole.

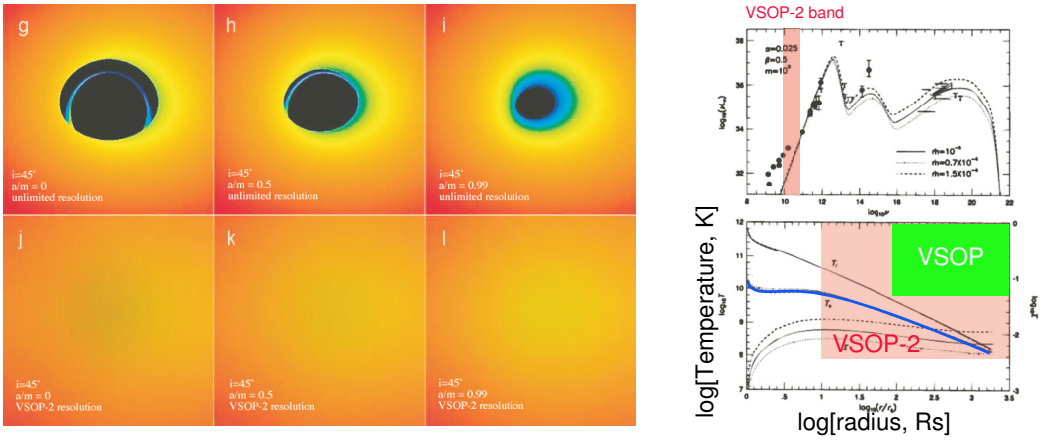

Fig. 1. (*Left*): Simulated black hole images of M 87. Upper and lower panels show the model and restored images with the VSOP-2 resolution, respectively (Takahashi 2004). (*Right*): Temperature distribution in an ADAF disk (Manmoto et al. 1997). The electron temperature is above the detection limit of the VSOP-2 within 1000 Schwarzschild radii.

Table 1. Candidates for direct images of an accretion disk

Name	D [Mpc]	$M_{\rm BH}$ [10^8 $M_\odot$]	θ_g [μas]	$S_{\rm 15GHz}$ [mJy]	Remarks
NGC 3031 (M 81) .	3.63	0.7	0.93	164.8	
NGC 3627	6.6	0.9	0.27	2.9	
NGC 3998	21.6	5.8	0.53	85	S at 5 GHz
NGC 4143	17	3.7	0.44	10	
NGC 4261	35.1	7.5	0.43	6230	S at 8.4 GHz
NGC 4278	9.7	2.8	0.57	89.7	
NGC 4374 (M 84) .	18.4	16	1.74	183.7	
NGC 4486 (M 87) .	16.8	32	3.81	2835.7	
NGC 4552	16.8	3.7	0.43	58.6	
NGC 4594 (M 104)	20	2.7	0.27	86.6	S at 8.4 GHz
NGC 5128 (Cen A)	4.2	2.4	2.96	2500	S at 8.4 GHz
IC 1459	27	25	1.85	1000	
SgrA*	0.008	0.04	6.50	1030	S at 8.4 GHz

1.2. Accretion Disks

Accretion disks are considered to be the power plant where gravitational energy of accreting matter converts to radiation and where jets are produced and accelerated. None of telescopes have ever succeeded to image accretion disks directly. Imaging study for accretion disks in AGNs is the most important and promising subject with the VSOP-2. The priority of VSOP-2 observations is to test the AGN paradigm — a system consists of a massive black hole and an accretion disk — by imaging study of the disk. Imaging studies also allow us to discriminate disk models by means of the size of accretion disks, distributions of temperature and surface density, and pattern of the magnetic fields. Since the size of an accretion disk is proportional to the Schwarzschild radius, nearby AGNs are the best candidates to be imaged.

There are three major models on accretion disks; the standard disk model (Shakura & Sunyaev 1973), the ADAF (Advection-Dominated Accretion Flows) (Narayan & Yi 1994), and the Slim disk model (Abramowicz et al. 1988). Physical properties of equilibrium condition in these models are summarized in Abramowicz et al. (1995). The effective temperatures of the standard and the slim disks are predicted as $\sim 10^{4-5}$ and $\sim 10^6$ K, respectively. Thus, black-body radiation from them are too faint to be detected with the VSOP-2, whose brightness sensitivity is $\sim 10^8$ K.

ADAF is radiatively inefficient so that the accreting gas is not cooled efficiently and becomes as hot as the virial temperature of $T_{\rm ion} \sim m_p c^2/k(r/r_s) = 10^{13}(r/r_s)^{-1}$ K for ions and $T_{\rm e} \sim m_e c^2/k(r/r_s) = 6{\times}10^9(r/r_s)^{-1}$ K. The condition is far from equilibrium because the gas is collisionless (Begelman & Chiueh 1988). Equivalence of the virial temperature and the gas temperature, or identically that of rotating speed and sound speed, makes geometrically thick ($H \sim r$) torus shape. Hence, the gas density must be thin. Most of low luminosity AGNs (LLAGNs) show spectral energy distributions (SEDs) which is expected from the ADAF model. LLAGNs are popular. About 40% of nearby galaxies host an LLAGN (Ho et al. 1997).

The resolution of the VSOP-2 is comparable to apparent sizes of accretion disks in nearby AGNs. Its synthesized beam of 38 μas at 43 GHz corresponds to 13 r_s for M 87, so that the image of the accretion disk can be resolved. Table 1 lists nearby (within 20 Mpc) AGNs whose accretion disks can be resolved by the VSOP-2. There are at least three objects in which the VSOP-2 beam size corresponds to sharper than 20 r_s, and at least 13 objects for 200 r_s within 20 Mpc from the earth.

1.3. Circumnuclear Region

Sub-pc region of AGNs, corresponding to $10^3 - 10^5$ Schwarzschild radii is a mass reservoir where accreting matter is accumulated in. Total mass and velocity fields in this region is tightly related with the mass accretion rate which is an important indicator of AGN activity. The physical phase of matter in the sub-pc region is complex. Some type-2 Seyfert galaxies, LINERs (Low-Ionization Narrow Emission line Region), and radio galaxies emit H_2O or OH masers, which are indicators of dense ($n_{\rm H} > 10^9$ cm^{-3}) warm ($T > 400$ K) molecular disks, from its sub-pc regions (Moran et al. 1999). VLBI observations of HI absorption revealed rotating neutral gas disk sized $\sim$ 10 pc (Mundell et al. 1995; Conway & Blanco 1995; Taylor 1996; Sawada-Satoh et al. 2000). Furthermore, a plasma torus or disk is found in 0.1 – 1 pc via free–free absorption (Walker et al. 2000; Jones et al. 2001; Kameno et al. 2001; Kameno et al. 2003). Besides radio observations, X-ray spectroscopy revealed dense cold matter named "warm absorber" in the vicinity of the central engine via soft X-ray absorption and OVII and OVIII edges (Krolik & Kriss 2001). Tanaka et al. (1995) detected broad iron fluorescent line in the Seyfert galaxy MCG -6-15-30. The line at 6.4 keV in the rest frame is spread and redshifted, indicating that cold matter does exist in < 10 r_s vicinity of the black hole where gravitational redshift is significant. These facts suggest that mixture of gas in multiple phases such as molecular, neutral, and plasma exist in the sub-pc region.

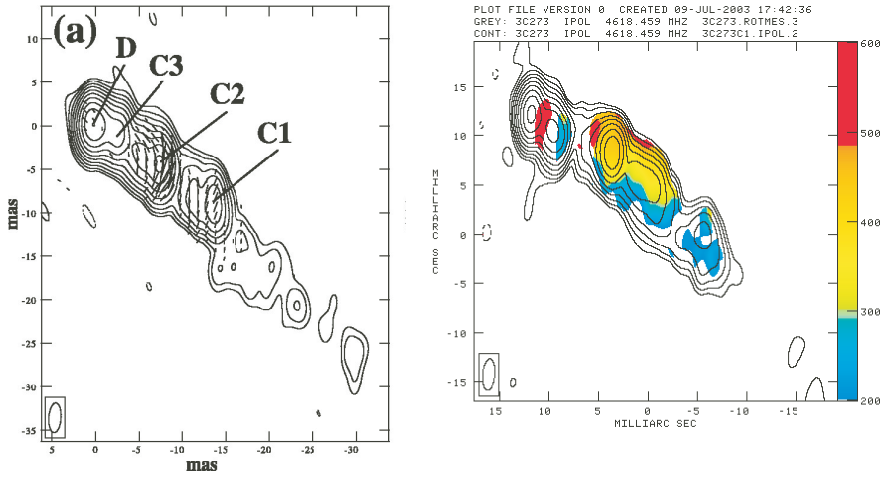

Fig. 2. Polarization observation of 3C 273 by Asada et al. (2002). (*Left*): E-vector in tick marks with the total intensity map in contour. (*Right*): Rotation measure in pseudo color. The gradient across the jet indicates helical magnetic structure.

VSOP-2 offers a potential to illustrate the mixture of multiple-phase gas in the sub-pc region. Ionized and dense molecular gases can be probed via free–free absorption and H_2O maser emission. Denser plasma in the heart of AGNs absorbs radio emission at higher frequencies, so that higher resolution at higher frequency is essential. And 22-GHz reception capability is essential for H_2O maser studies. VSOP-2 is the best suited telescope which works at millimeter wavelengths and offers a resolution better than 100 μas corresponding to 0.01 pc in nearby AGNs. Precise distributions of gas will be a key to solve the question: what is the ionizing source, supernovae in the molecular disk, photoionization caused by secondary UV radiation, or direct X-ray radiation from the central engine.

1.4. Jets

It is still unclear what and how does accelerate AGN jets to the relativistic speed whose Lorentz factors are up to $\sim$ 30. Mainly three types of models are proposed for this mechanism; (1)MHD (Magneto-Hydrodynamics), (2)radiative pressure, and (3)shocks. In the MHD model, magnetic fields penetrating the accretion disk are twisted and form a helical structure to collimate and accelerate the jets by magnetic centrifugal force or magnetic pressure. It is an attractive model which can explain both collimation and acceleration mechanisms. The radiative pressure model (Bisnovatyi-Kogan & Blinnikov 1977) explains that thermal radiation of the accretion disk accelerates pair-plasma particles (positrons and electrons) created near the black hole. Geometrically thick configuration is essential to collimate the jet and to avoid radiative drag (Fukue & Umemura 1995). Shock can also contribute to particle acceleration. In the Fermi acceleration process, particles gain their energy through round-trip movements between two flows at different velocities. In the case of AGN jets, shock acceleration occurs when following fast flow collides with preceding slow flow (Kataoka 2004). The gain is proportional to number of movements, whose chance probability obeys the power-law. Hence, the power-law spectra is naturally explained.

High resolution capabilities of the VSOP-2 will clarify details of fine structures of jets, such as shock fronts or filaments along the magnetic fields, in the acceleration and collimation region. It is remarkable that VSOP-2 offers polarization imaging capabilities. Since E-vector of optically thin synchrotron emission is perpendicular to the magnetic field, linear polarization map tells us magnetic field structures projected in the plane of the sky. Furthermore, Faraday rotation measure is a powerful tool to investigate magnetic field along the line of sight. Combination of the polarization map and Faraday rotation measure will be a clue of three-dimensional magnetic structures, as was demonstrated by Asada et al. (2002).

2. Protostars

Star formation is a mass contraction process from mother molecular clouds to protostars. Density fluctuations in the molecular cloud enhances by the self gravity to form a dense core. Densest fragments contract into a class-0 protostar and a protoplanetary disk surrounding it. The protostar grows as materials of the disk accretes onto it until nuclear fusion stars.

The accretion processes in various stages are investigated with different types of resolutions: single-dish radio telescopes for molecular clouds, mm-wave interferometers for disk envelopes, and ground-based VLBI for protoplanetary disks and outflows. Besides these telescopes, space VLBI is capable to resolve the final stage of accretion from a disk onto a protostar.

Recent observational and theoretical studies indicate that a magnetosphere associates with YSOs (Andre 1996). It concerns magnetic connection between the protostar and the disk, regulation of disk angular momentum, and acceleration of outflows. X-ray flares are considered to be powered in the magnetospheres (Tsuboi et al. 2000). Non-thermal radio emission from YSOs is also a probe of the magnetospheres. The tight correlation between the radio luminosity and the X-ray luminosity indicates

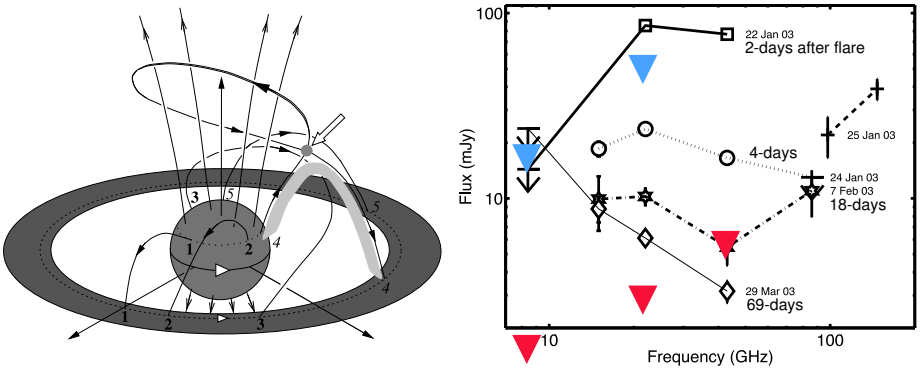

Fig. 3. (*Left*): X-ray flare model of YLW 15 (Montmerle et al. 2000). Magnetic fields connecting the protostar and inner edge of disk are twisted by the stellar rotation, and periodic reconnection causes X-ray flares. (*Right*): Radio spectra of Orion GMR-A after a flare (Bower et al. 2003). Blue and red triangles indicate detection limits of VSOP-2 without and with phase referencing capability, respectively.

that there is a common emission mechanism. Some protostars show signs of giant magnetospheres; such as circular polarization (Feigelson et al. 1998) and hard X-ray flares. Periodic X-ray flares can be a response of magnetic reconnection caused by rotation of the protostar. Gigantic flares at mm-waveband arise just after X-ray flares (Bower et al. 2003), showing inverted and steep spectra at rising and delaying phases, respectively. These results indicates that gyrosyncrotron radiation is the origin of mm-wave emission.

We aim to illustrate the magnetospheres of YSOs with the VSOP-2. The 38-μas resolution corresponds to 1.2 solar radius at the distance of nearby starforming regions ($d \sim 150$ pc). Since the magnetosphere has a dimension of a few tens of solar radii, VSOP-2 offers sufficient resolving power for this region. Interaction between inner edge of the protoplanetary disk and the protostar can be probed. Polarization capability allows us to image the magnetic fields in connecting the protostar and the disk.

Figure 3 shows radio spectra of Orion GMR-A at 2, 4, 18, and 69 days after a giant flare. The inverted spectrum just after the flare indicates that the emission region is optically thick at low frequencies. Thus, frequencies above 22 GHz is crucial to resolve magnetospheres. This figure also shows that phase referencing technique is essential to enhance the sensitivity. It enables monitoring for 70 days after a flare event.

References

Abramowicz, M. A., Chen, X., Kato, S., Lasota, J., & Regev, O. 1995, ApJ, 438, L37
Abramowicz, M. A., Czerny, B., Lasota, J. P., & Szuszkiewicz, E. 1988, ApJ, 332, 646
Andre, P. 1996, ASP Conf. Ser. 93: Radio Emission from the Stars and the Sun, 93, 273
Asada, K., Inoue, M., Uchida, Y., Kameno, S., Fujisawa, K., Iguchi, S., & Mutoh, M. 2002, PASJ, 54, L39
Begelman, M. C., & Chiueh, T. 1988, ApJ, 332, 872
Bisnovatyi-Kogan, G. S., & Blinnikov, S. I. 1977, A&A, 59, 111
Bower, G. C., Plambeck, R. L., Bolatto, A., McCrady, N., Graham, J. R., de Pater, I., Liu, M. C., & Baganoff, F. K. 2003, ApJ, 598, 1140
Conway, J. E., & Blanco, P. R. 1995, ApJ, 449, L131
Feigelson, E. D., Carkner, L., & Wilking, B. A. 1998, ApJ, 494, L215
Fukue, J., & Umemura, M. 1995, PASJ, 47, 429
Ho, L. C., Filippenko, A. V., Sargent, W. L. W., & Peng, C. Y. 1997, ApJS, 112, 391
Jones, D. L., Wehrle, A. E., Piner, B. G., & Meier, D. L. 2001, ApJ, 553, 968
Kameno, S., Inoue, M., Wajima, K., Sawada-Satoh, S., & Shen, Z. 2003, Publications of the Astronomical Society of Australia, 20, 134
Kameno, S., Sawada-Satoh, S., Inoue, M., Shen, Z., & Wajima, K. 2001, PASJ, 53, 169
Kameno, S., Inoue, M., Fujisawa, K., Shen, Z., & Wajima, K. 2000, PASJ, 52, 1045
Kataoka, J. 2004, Progress of Theoretical Physics Supplement, 155, 351
Krolik, J. H., & Kriss, G. A. 2001, ApJ, 561, 684
Manmoto, T., Mineshige, S., & Kusunose, M. 1997, ApJ, 489, 791
Montmerle, T., Grosso, N., Tsuboi, Y., & Koyama, K. 2000, ApJ, 532, 1097
Moran, J. M., Greenhill, L. J., & Herrnstein, J. R. 1999, Journal of Astrophysics and Astronomy, 20, 165
Mundell, C. G., Pedlar, A., Baum, S. A., O'Dea, C. P., Gallimore, J. F., & Brinks, E. 1995, MNRAS, 272, 355
Narayan, R., & Yi, I. 1994, ApJ, 428, L13
Sawada-Satoh, S., Inoue, M., Shibata, K. M., Kameno, S., Migenes, V., Nakai, N., & Diamond, P. J. 2000, PASJ, 52, 421
Shakura, N. I., & Sunyaev, R. A. 1973, A&A, 24, 337
Takahashi, R. 2004, ApJ, 611, 996
Tanaka, Y., et al. 1995, Nature, 375, 659
Taylor, G. B. 1996, ApJ, 470, 394
Tsuboi, Y., Imanishi, K., Koyama, K., Grosso, N., & Montmerle, T. 2000, ApJ, 532, 1089
Walker, R. C., Dhawan, V., Romney, J. D., Kellermann, K. I., & Vermeulen, R. C. 2000, ApJ, 530, 233